

Progress of HL-2A Experiment and HL-2M Program

Xuru Duan

on behalf of SWIP and collaborators

Southwestern Institute of Physics, Chengdu, China

28th IAEA Fusion Energy Conference, 10-15th, May, 2021.



Outline

- Introduction
- Progress of HL-2A Experiment
 - High β_N operation
 - Impurity effect on transport and confinement
 - L-H transition and ELM mitigation
 - Energetic particle and MHD instability
- HL-2M Program
 - Mission
 - First plasma
 - Auxiliary System
- Summary



Introduction

Fusion research activities at SWIP :

- Tokamak program (HL-2A & HL-2M)
Including Engineering, Experiments, Theory & Simulation

- Fusion reactor design

- Fusion technology relevant activities:

Fusion reactor materials

R&D of key components (advanced divertor,....)

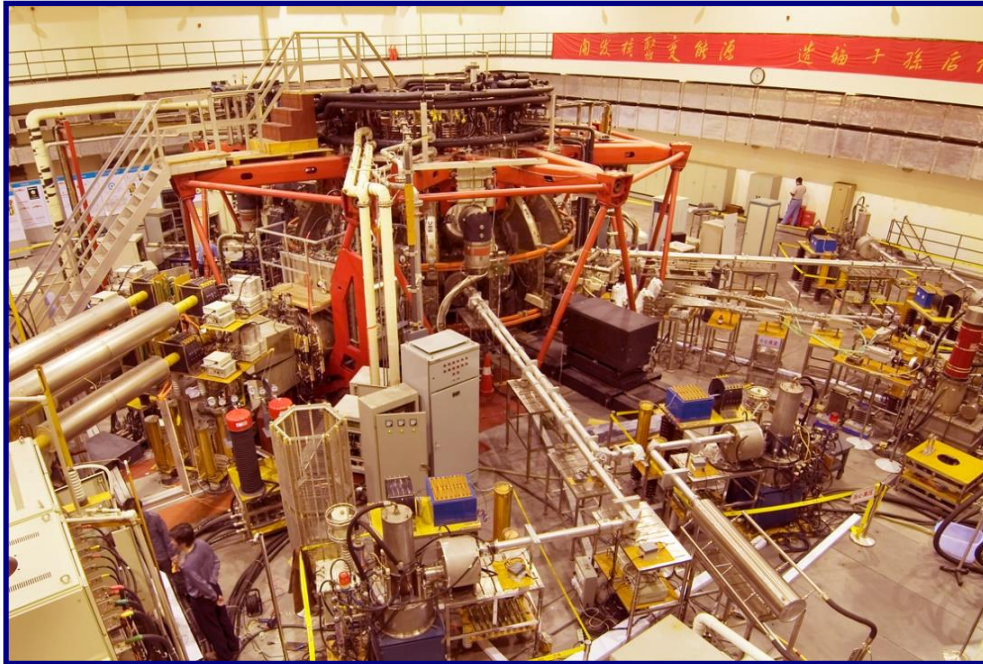
R&D of ITER Procurement Packages at SWIP

Helium-cooled solid breeder test blanket module (TBM)

- First Wall & Shielding Blanket
- Gas Injection & Glow Discharge Cleaning System
- Magnet Support
- Neutron Flux Monitoring
- Langmuir Probe



HL-2A Tokamak



R : 1.65 m

a : 0.40 m

B_T : 1.2~2.7 T

Configuration:

Limitor, LSN divertor

I_p : 150 ~ 480 kA

Auxiliary heating:

ECRH/ECCD: 5 MW

(6 X 68 GHz/0.5 MW/1 s,

2 X 140 GHz/1 MW/1 s)

NBI (tangential): 3 MW

LHCD: 2 MW (4/3.7 GHz/0.5 MW/2 s)

Fueling system (H_2/D_2):

Gas puffing (LFS, HFS, divertor)

Pellet injection (LFS, HFS)

SMBI (LFS, HFS)

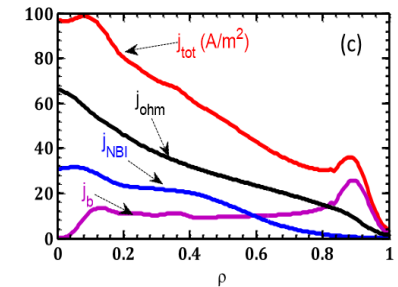
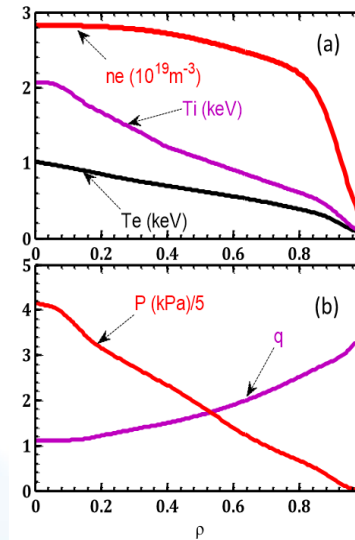
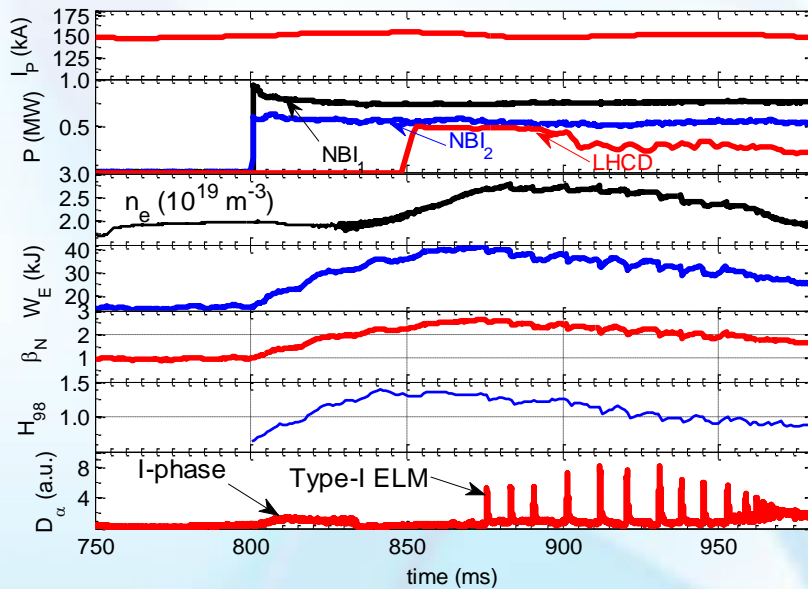
LFS: $f = 1 \sim 80$ Hz, pulse duration > 0.5 ms

gas pressure < 3 MPa

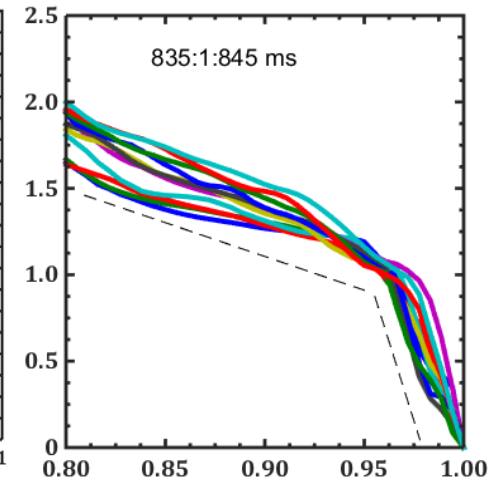
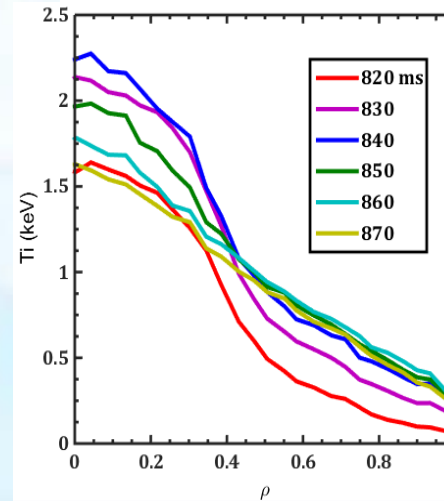


High- β_N Operation

- Integrated modeling for high β_N exp.
- Two NBI systems for high performance operation
- Appropriate configuration and heating power deposition
- Hybrid scenarios with double transport barriers achieved.
- $\beta_N > 2$ with duration $\sim 15\tau_E$



Simulations by OMFIT for HL-2A exp.

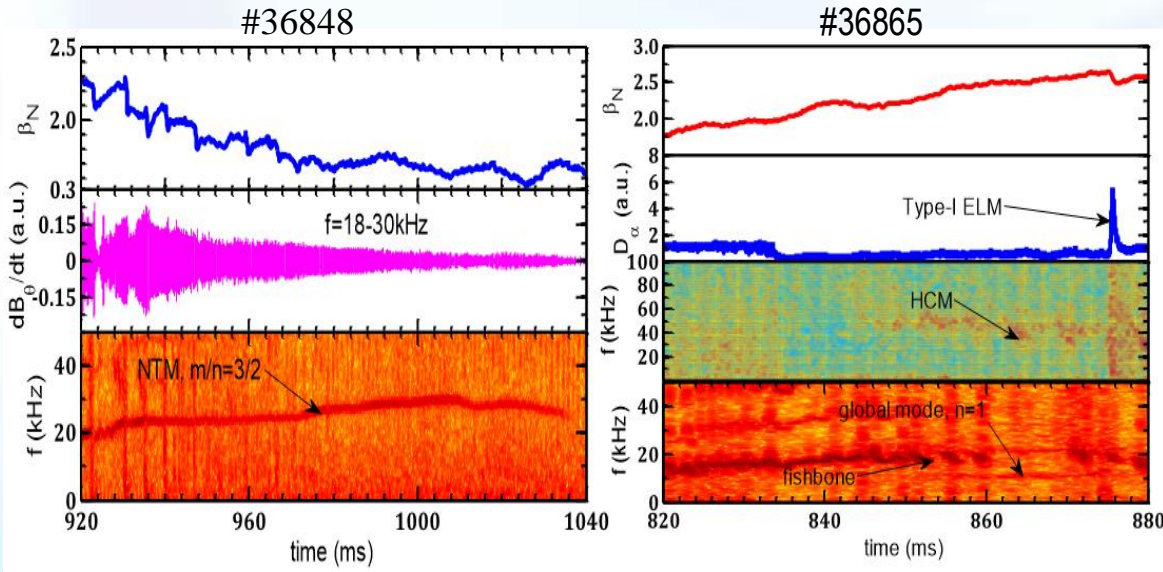
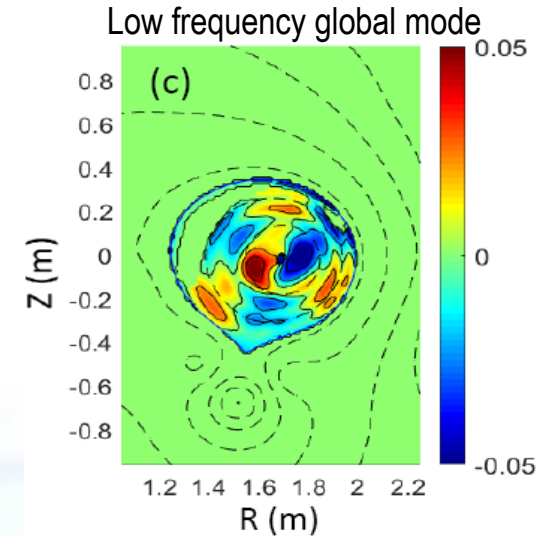


W. Chen, this conference



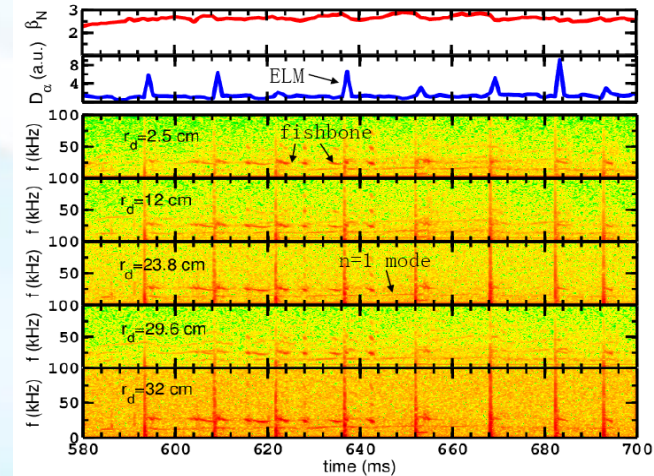
MHD Instabilities in High- β_N Plasmas

- High-frequency coherent mode was induced by LHCD. Strong electrostatic fluctuation components, $k_\theta \sim 1.4 \text{ cm}^{-1}$, can regulate particle and energy transport.
- Low frequency global mode: coupling of destabilized internal and external modes with $m/n=1/1$ and $m/n=3/1$, respectively. \rightarrow Playing a critical role in the triggering onset of ELMs.
- NTM: $m/n=3/2$, $f \sim 25 \text{ kHz}$



NTM

High frequency global mode

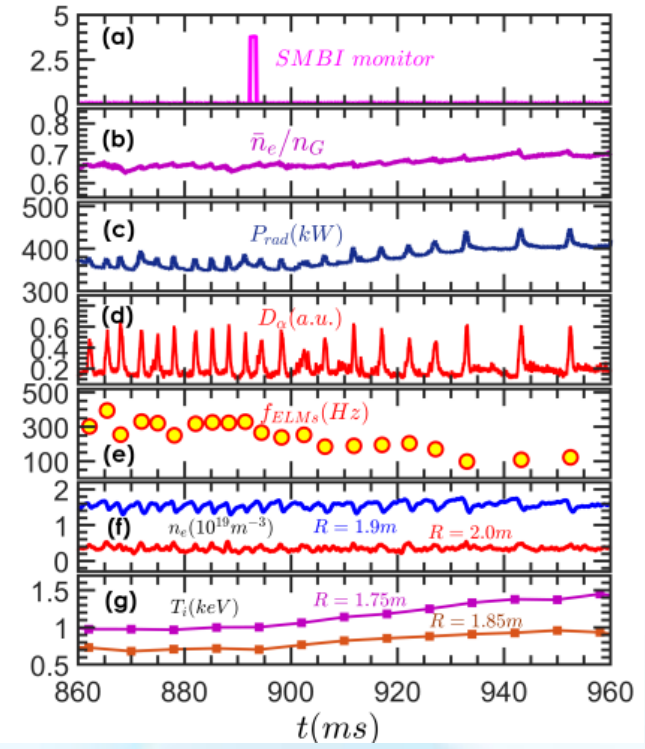
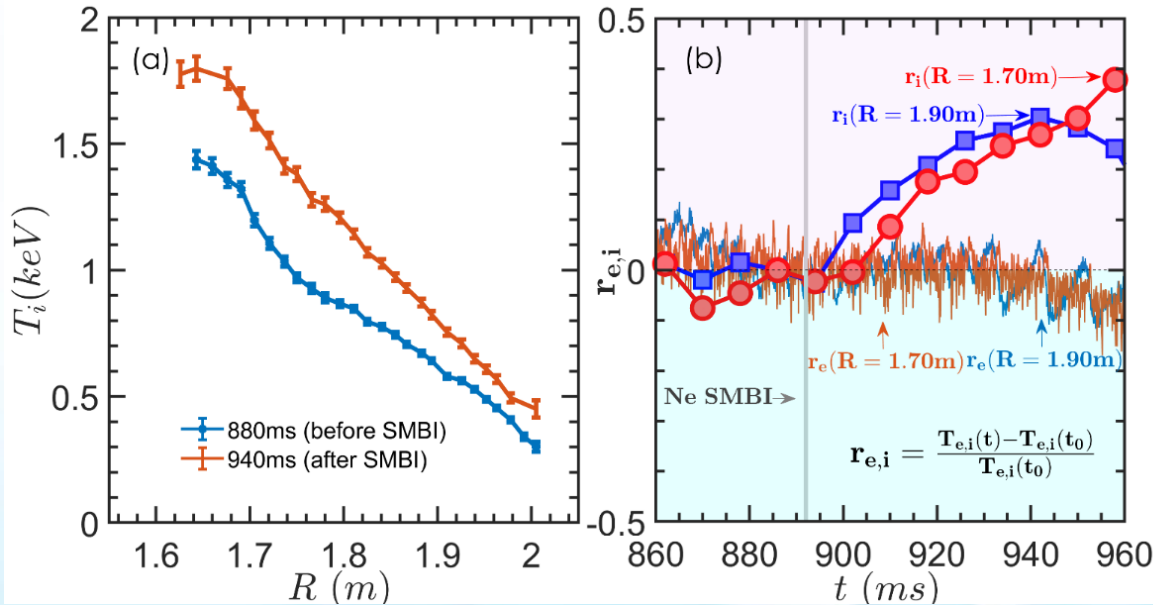


W. Chen, this conference



Confinement Enhancement with Impurity Seeding

- H-mode confinement is improved by neon impurity seeding in the ELMy H-mode
- Ion and electron heat flux exhibits distinct responses to the impurity seeding.
- Electron and ion thermal transports are decoupled by the impurity seeding.
- Decoupled ion thermal transport contributes to an improved energy confinement.

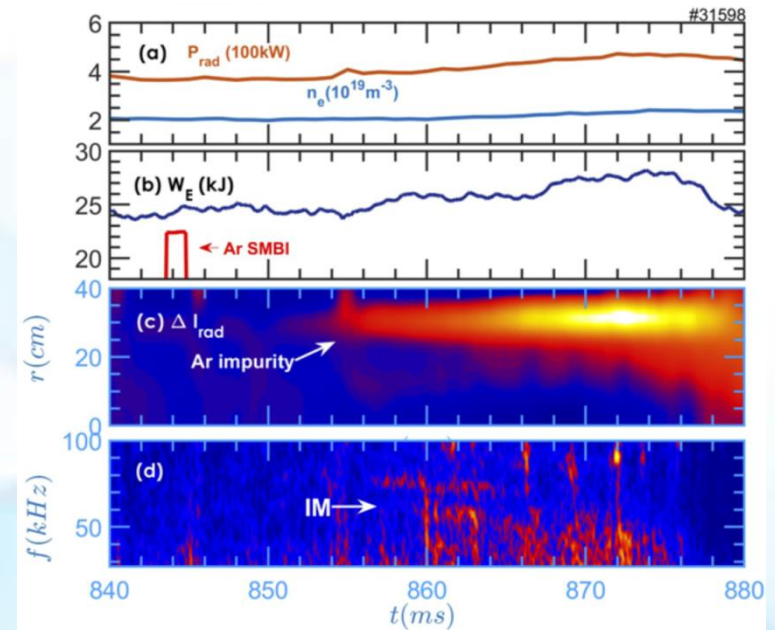
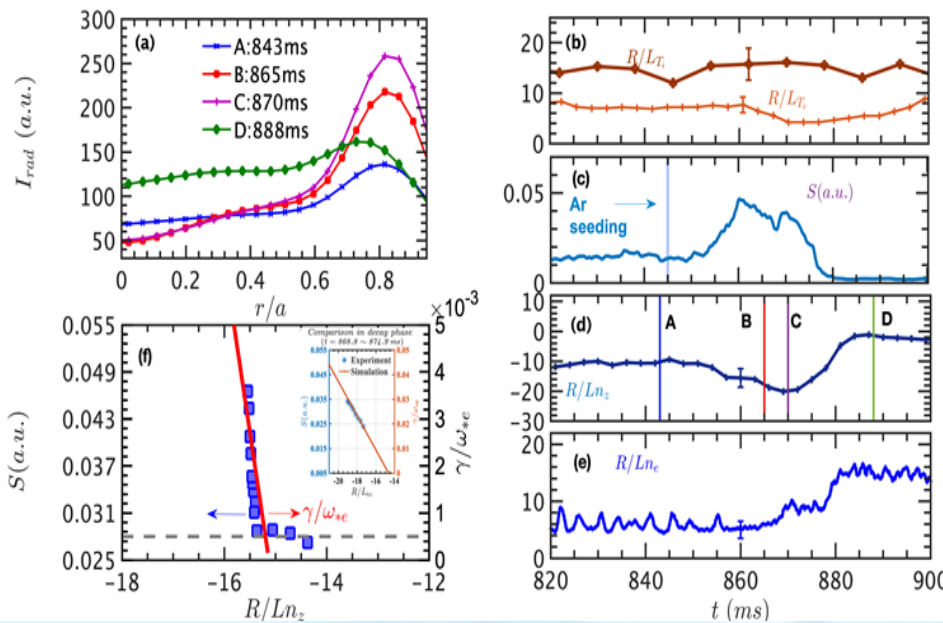


W.L. Zhong, this conference



Impurity Transport and its Te Screening Effect

- The evidences of impurity mode induced transport such as impurity density peaking factor (PF) are observed in argon injection experiment for the first time.
- Theory predicted ITG screening effects on the transport are evidenced in the experiment.
- The increment of R/L_{ne} plays a key role in the decrement of PF and sustainment of slightly hollow profile of impurity ions.

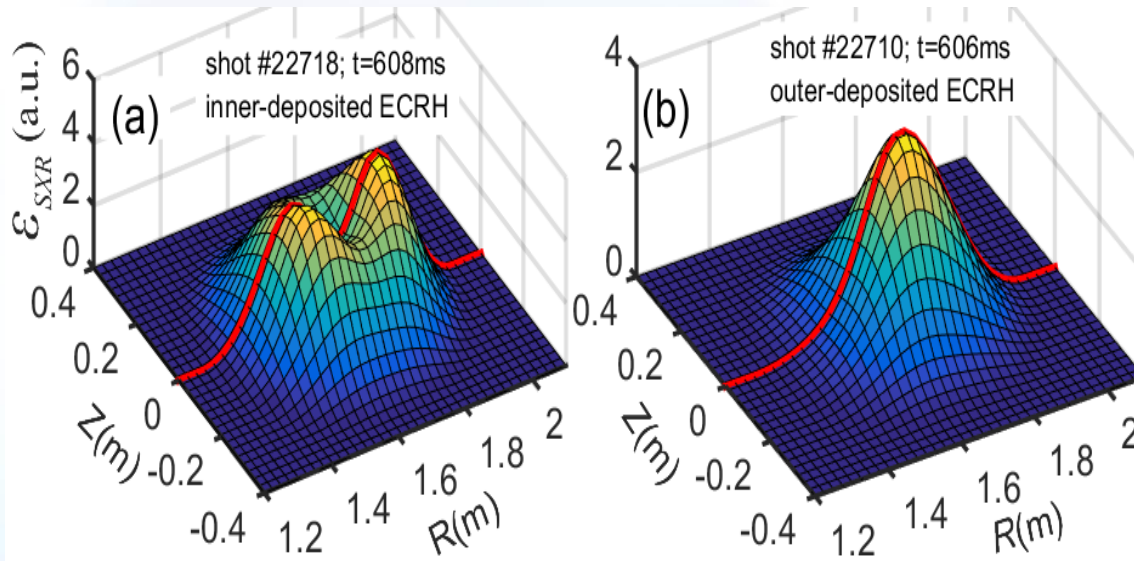


M.K. Han, NF 2021



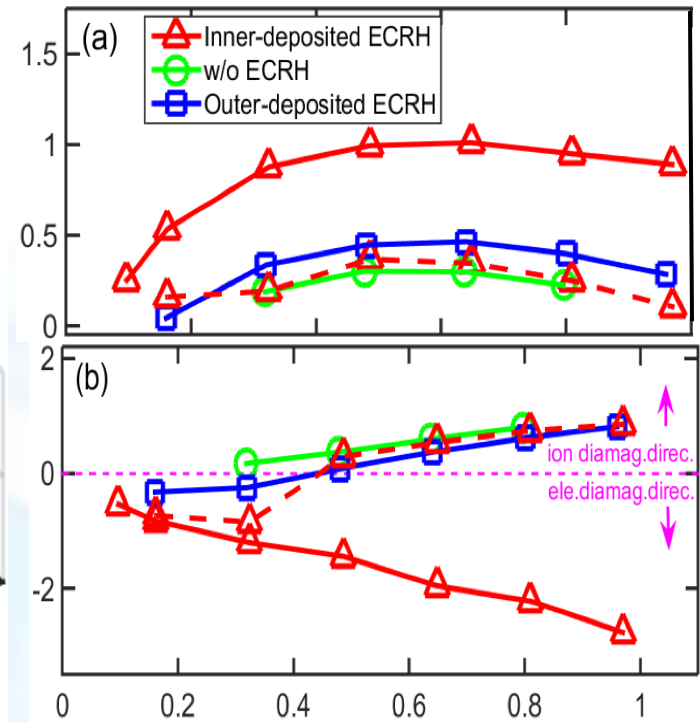
Impurity Transport and TEM Turbulence

The strongly hollow impurity density profile observed in experiments arises from the combined effect of the expulsion of impurity by MHD instability in the plasma center and an inward impurity convection driven by TEM turbulence in the outer confinement region.



Soft X-ray reconstructions after the injection of Al impurity in discharges with (a) inner- and (b) outer-deposited ECRH.

Identification of the unstable modes by the spectra of the (a) growth rate and (b) real frequency



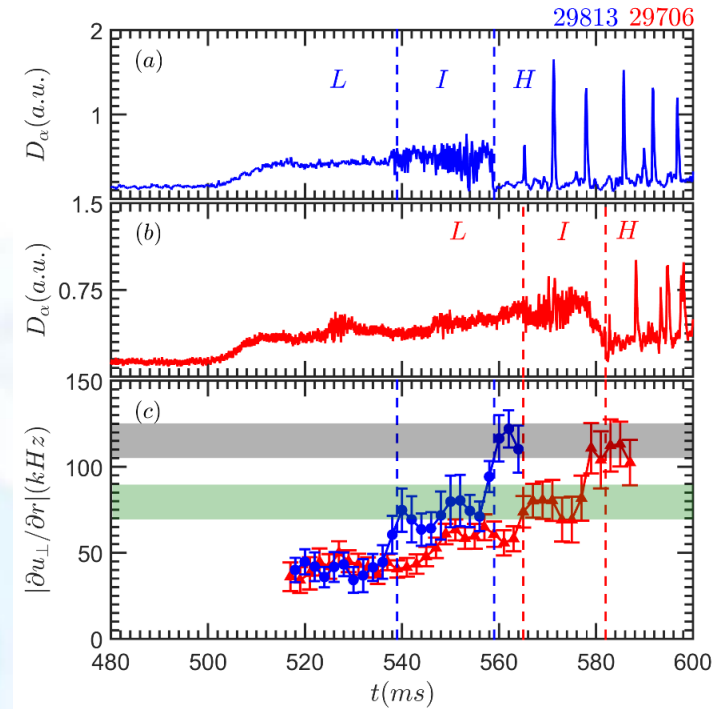
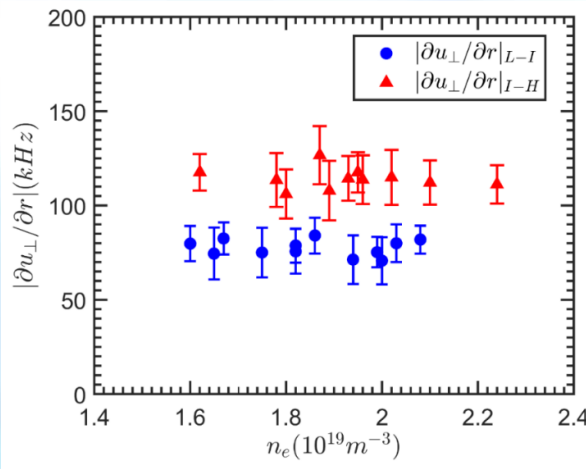
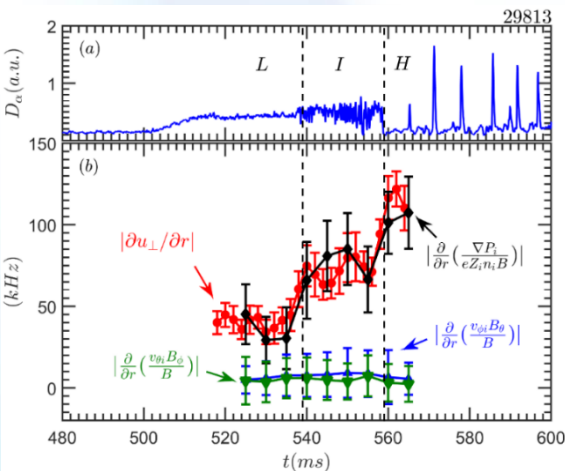
D. Li, NF 2020



Edge Velocity Shear for L-I-H Transition

Threshold of Edge Velocity Shear for L-I-H Transitions

- Velocity shear increases before the L-I and L-H transitions. Significant decrease of turbulence and increase of density gradient were observed at the L-H transition, mainly due to the pressure gradient term
- L-H transition occurred only when the velocity shear exceeded some threshold, which is independent of the plasma density or the heating power.



A.S. Liang, NF 2020



Effect of SMBI on L-H transition

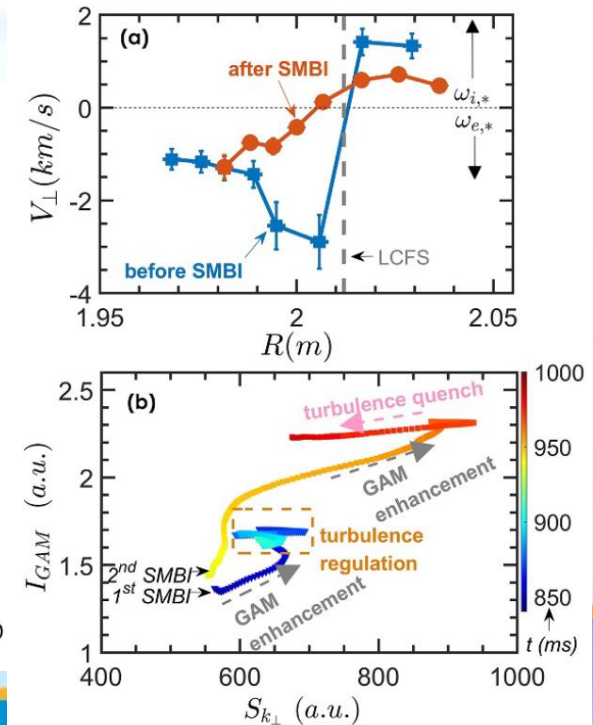
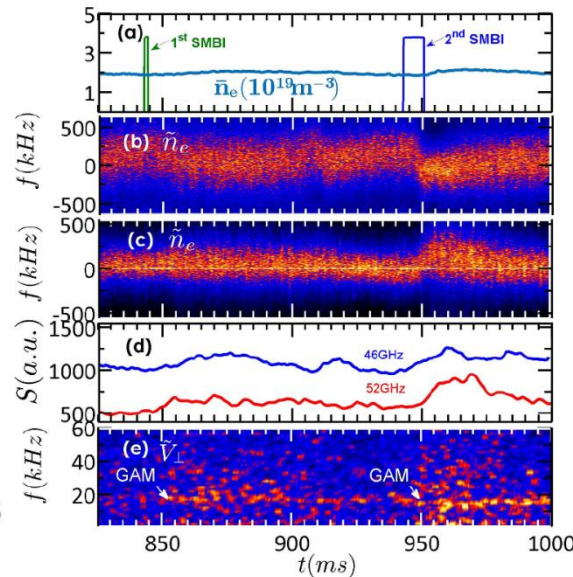
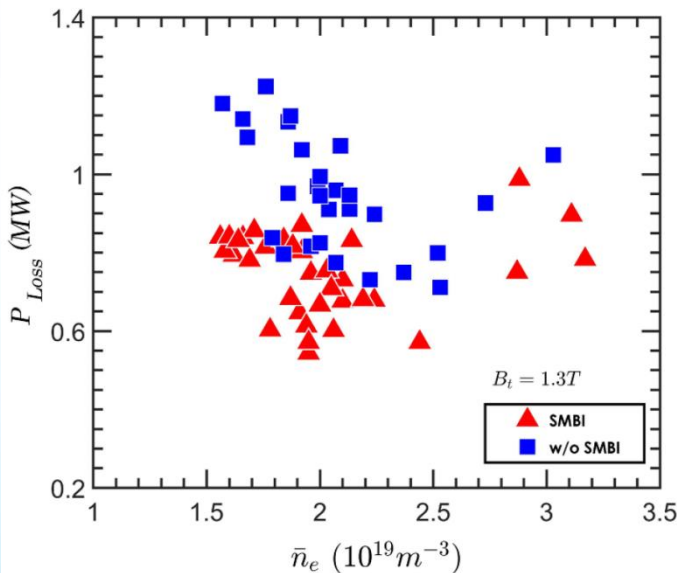
- Mechanism of SMBI on L-H transition is demonstrated.

Two dynamic processes:

GAM intensity increases with the turbulence intensity owing to the SMBI

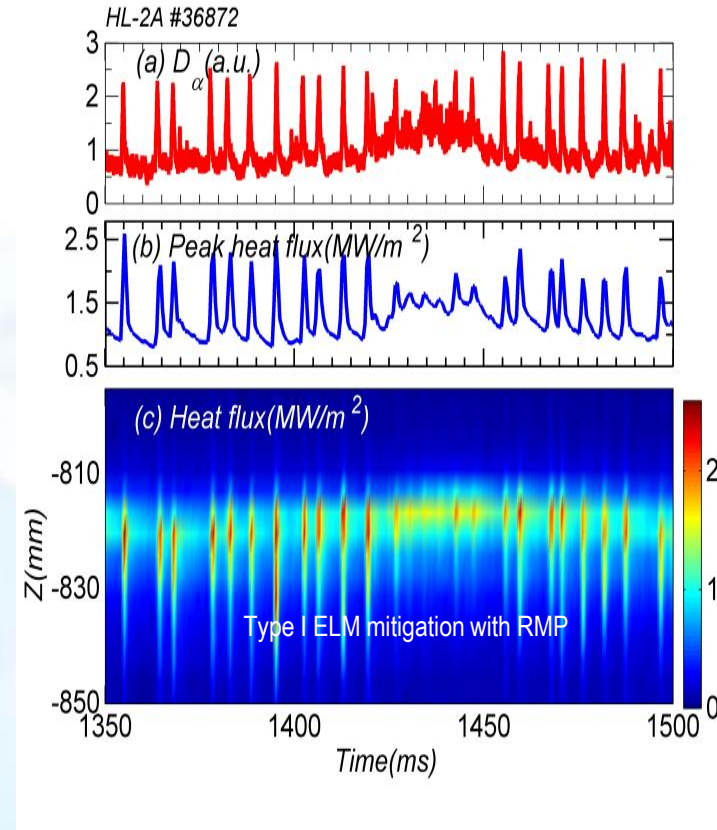
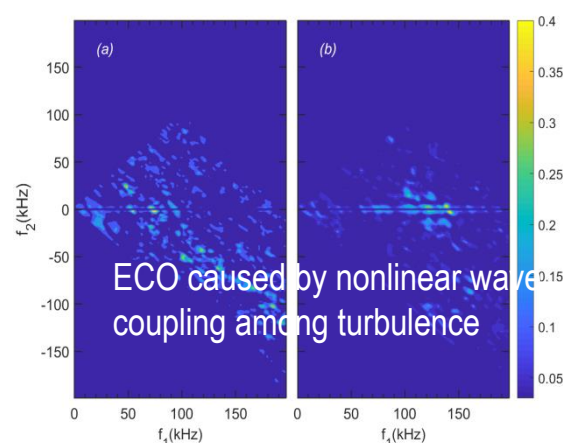
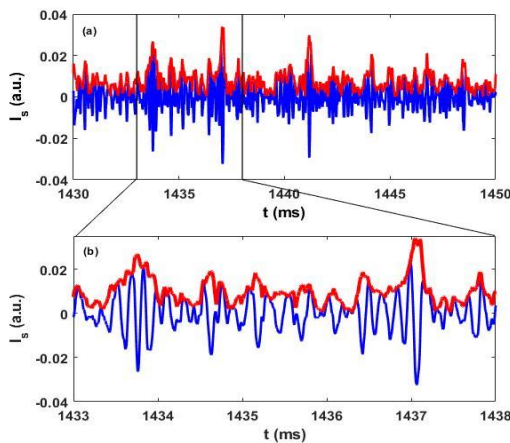
Interaction between GAM and turbulence indicates that the turbulence is quenched by the GAM

- Nonlinear regulation dynamics between the turbulence and shear flows is externally enhanced by SMBI. The enhancement plays a key role in facilitating the L-H transition.



Mechanism of ELM Mitigation by RMP

- Edge coherent oscillation (2–25 kHz), caused by the *three-wave interaction of turbulence* enhanced by RMP, is observed in the steep-gradient pedestal region of ELM mitigated H-mode plasmas.
- The mode drives a significant outflows of particles and heat, providing a channel for continuous particle transport across the pedestal during the mitigation of ELM.

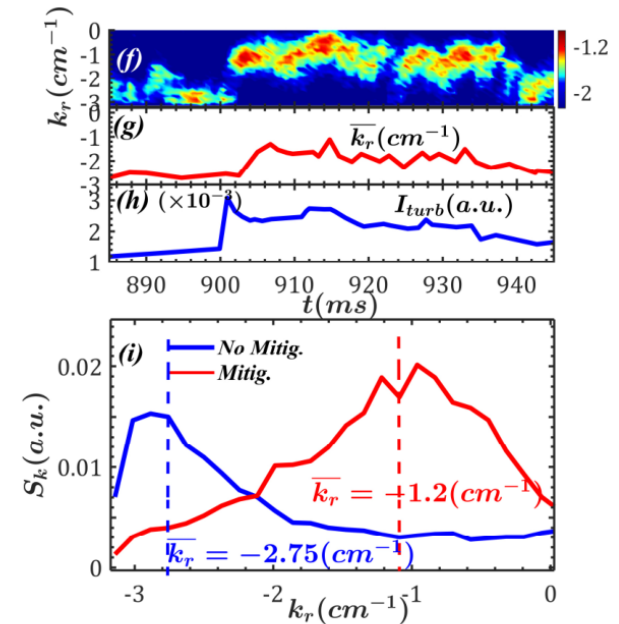
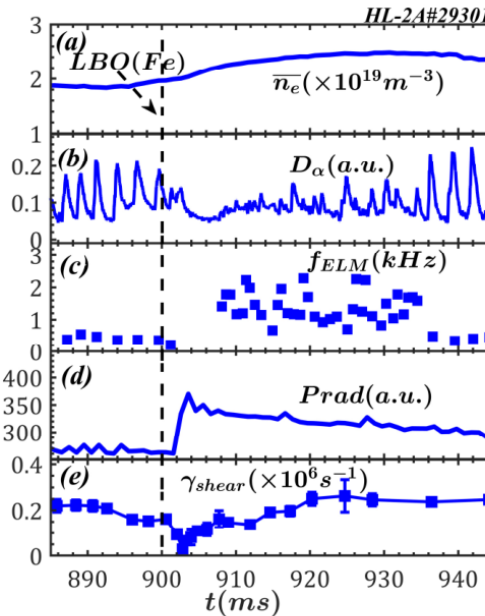
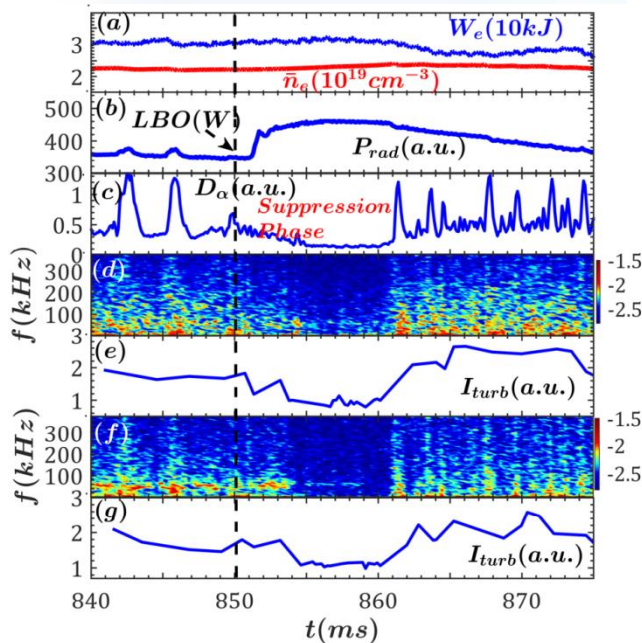


ECO induced continuous particle transport

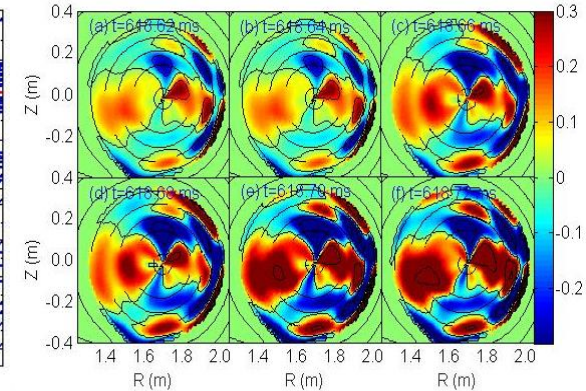
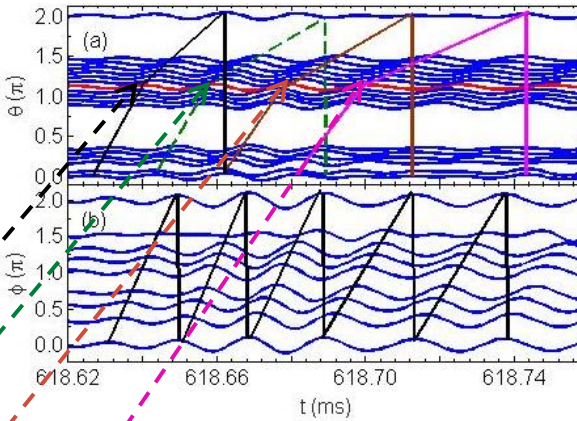
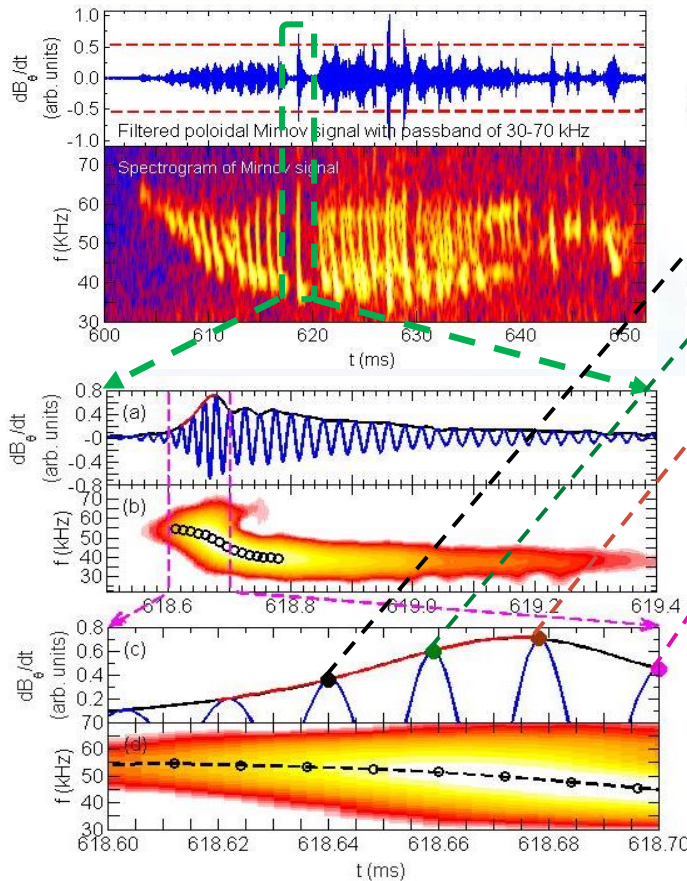


LBO Impurity Seeding for ELM Mitigation

- ELM mitigation and suppression has been achieved by LBO impurity seeding.
- Pedestal turbulence is governed by the turbulence wavenumber shift process.
- Dual effect of the impurity on the turbulence behavior interact in the pedestal, result in the turbulence enhancement during ELM mitigation and turbulence suppression during ELM suppression



Evidence of EPM Avalanche Dynamics



- In a successive chirping process (a strong single burst) $t=618.60-618.76$ ms:
 - The frequency of the mode sweeps down from 55 to 43 kHz;
 - Poloidal mode number changes from $m=2$ to 3, and then from 3 to 4.
 - Toroidal mode number keeps at $n=1$.
- Additionally, radial propagation of EPM can also be proved by:
 - $m=2$ elements are dominant at first, then the mode propagates in outward. At last, the $m=4$ elements are dominant.

L.M. Yu, submitted to NF 2021

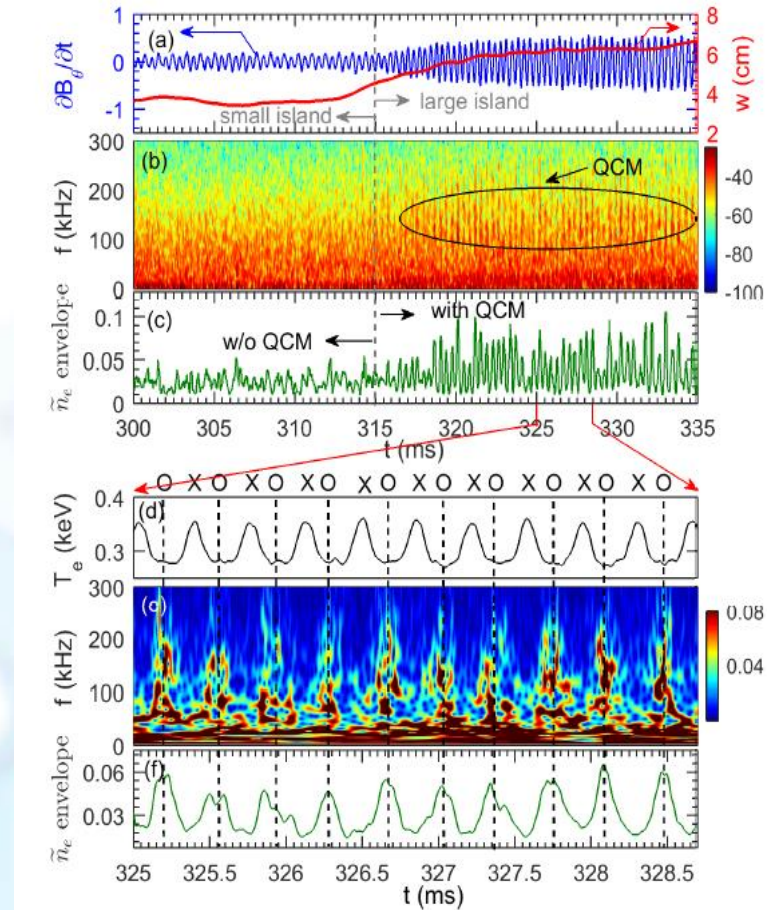
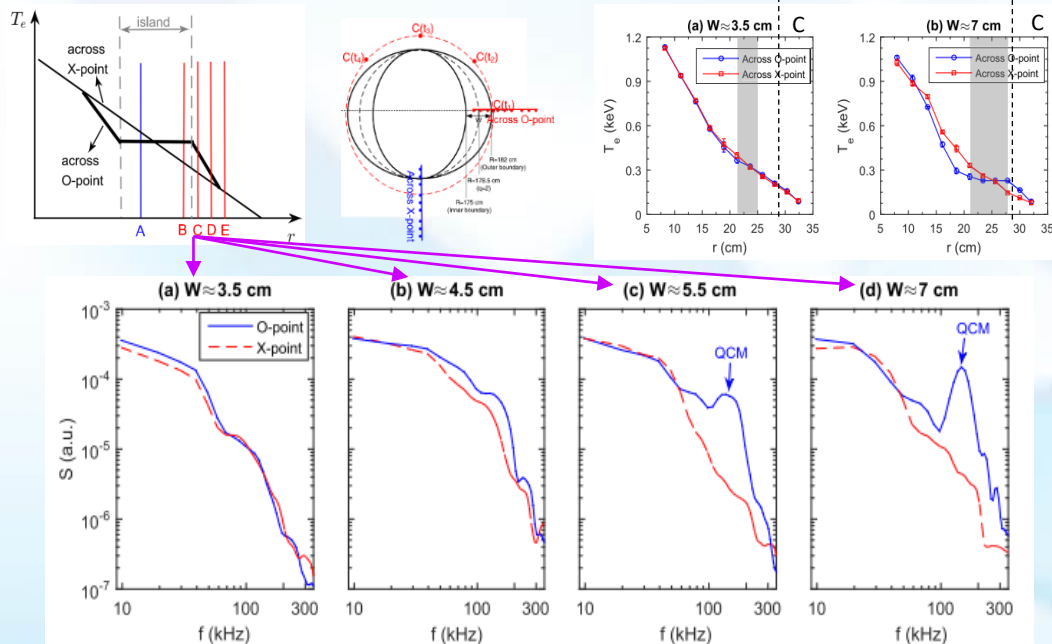


Influence of Large Magnetic Island Structures

Influence of large magnetic island structures on turbulence and quasi-coherent modes

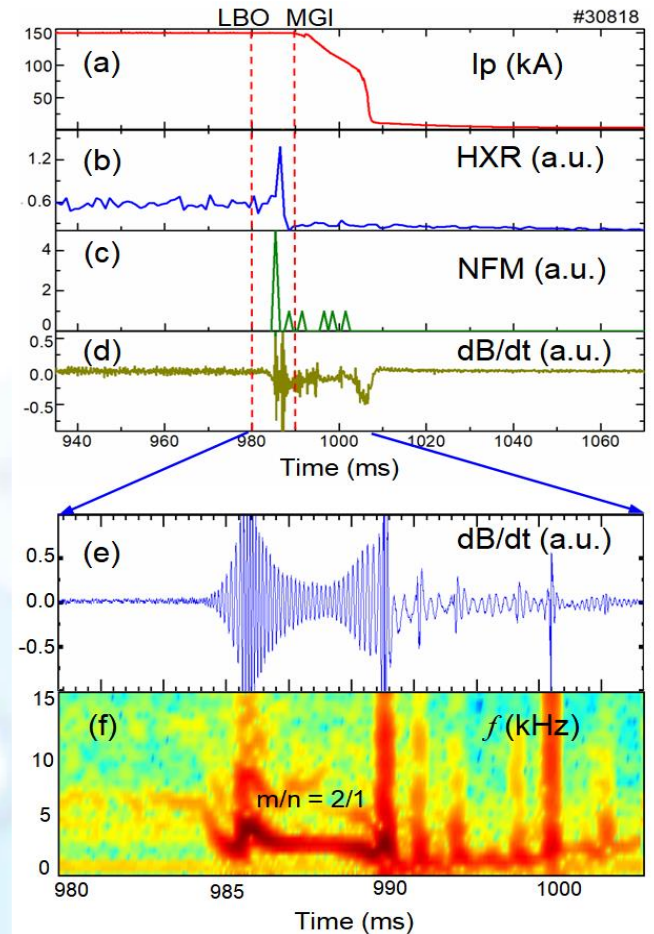
The influence of the rotating $m/n = 2/1$ magnetic islands:

- Both the QCM (100–175 kHz) and broadband turbulence (40–100 kHz and 175–300 kHz) outside the island are significantly enhanced during the O-point phase in comparison with that of the X-point.
- The QCM magnitude increases with the island size.

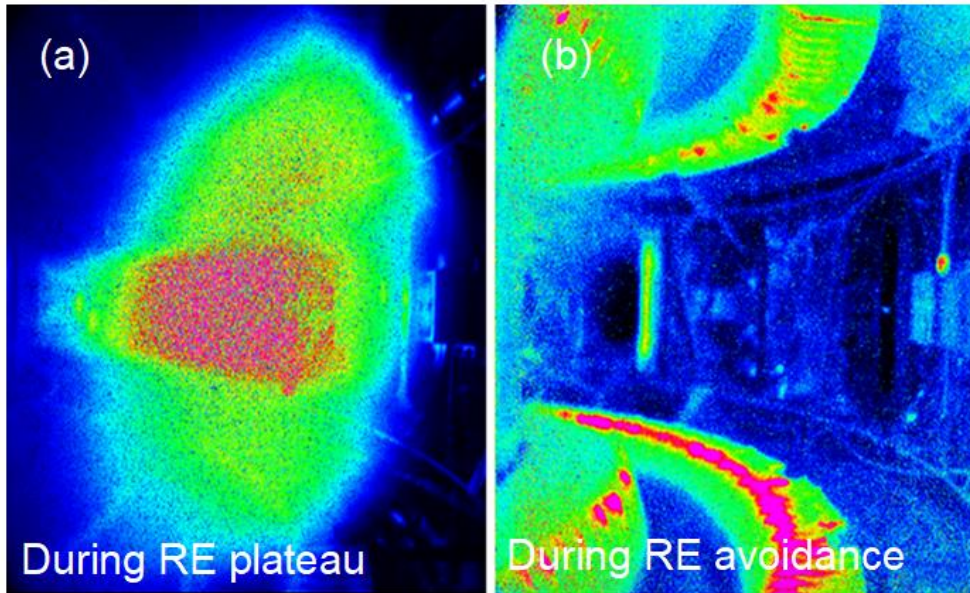


LBO for Disruption Mitigation

- With LBO system, the avoidance of runaway current generation during disruptions has been successfully achieved.
- With the impurity injection, strong $m/n=2/1$ mode was excited about 5 ms after LBO.
- The 'seed' electrons for the runaway current are 'killed' by strong magnetic fluctuation.

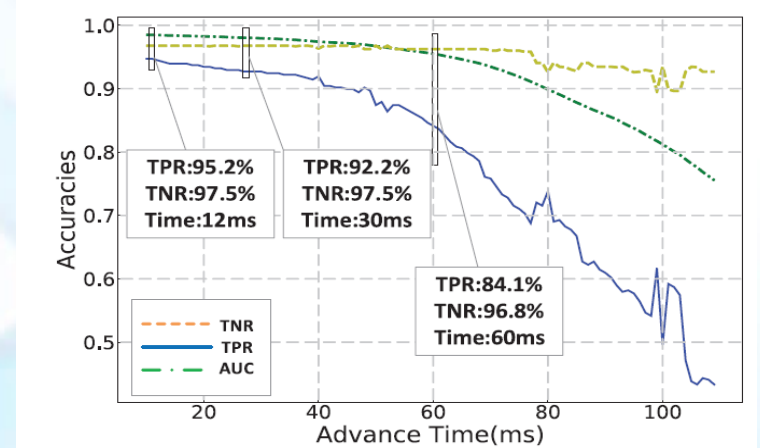
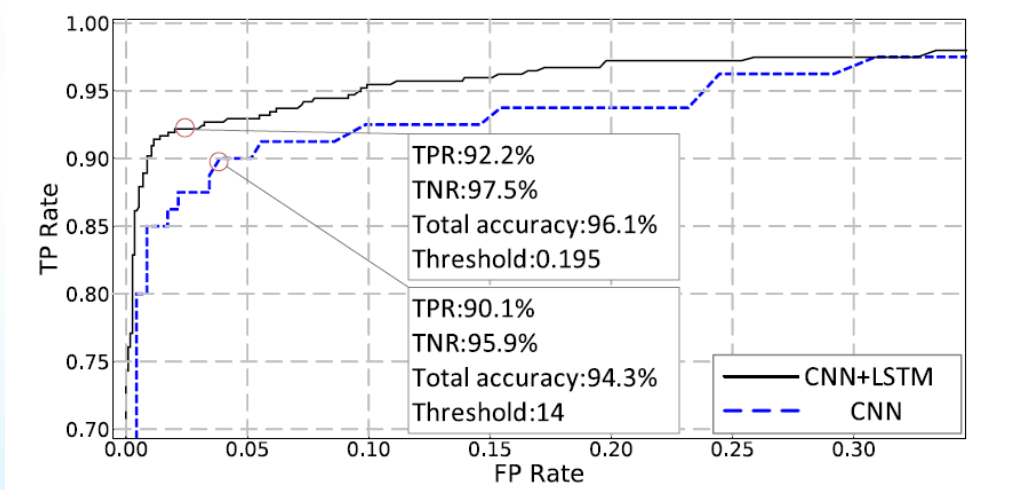
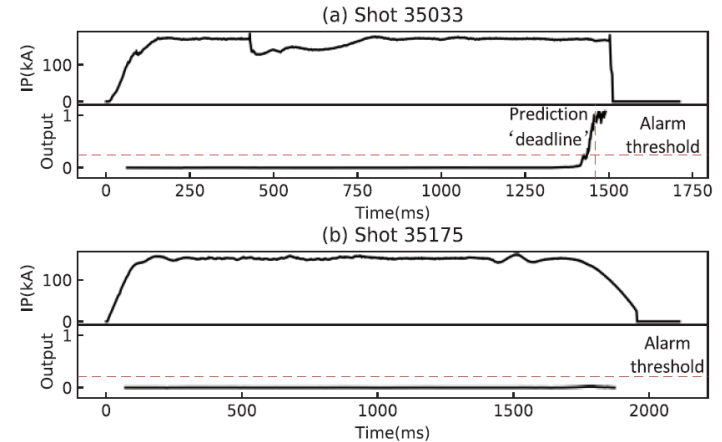


Y.P. Zhang, this conference



Disruption Predicted by Deep Learning

- Disruption prediction algorithms developed based on deep learning.
- Accuracy: 96.8%, by assembling convolutional neural network (CNN) and long short-term memory (LSTM) neural network.
- Disruption alarms : 30 ms before current quench.



Z.Y. Yang, this conference



Outline

- Introduction
- Progress of HL-2A Experiment
 - High β_N operation
 - Impurity effect on transport and confinement
 - L-H transition and ELM mitigation
 - Energetic particle and MHD instability
- **HL-2M Program**
 - **Mission**
 - **First plasma**
 - **Auxiliary System**
- **Summary**



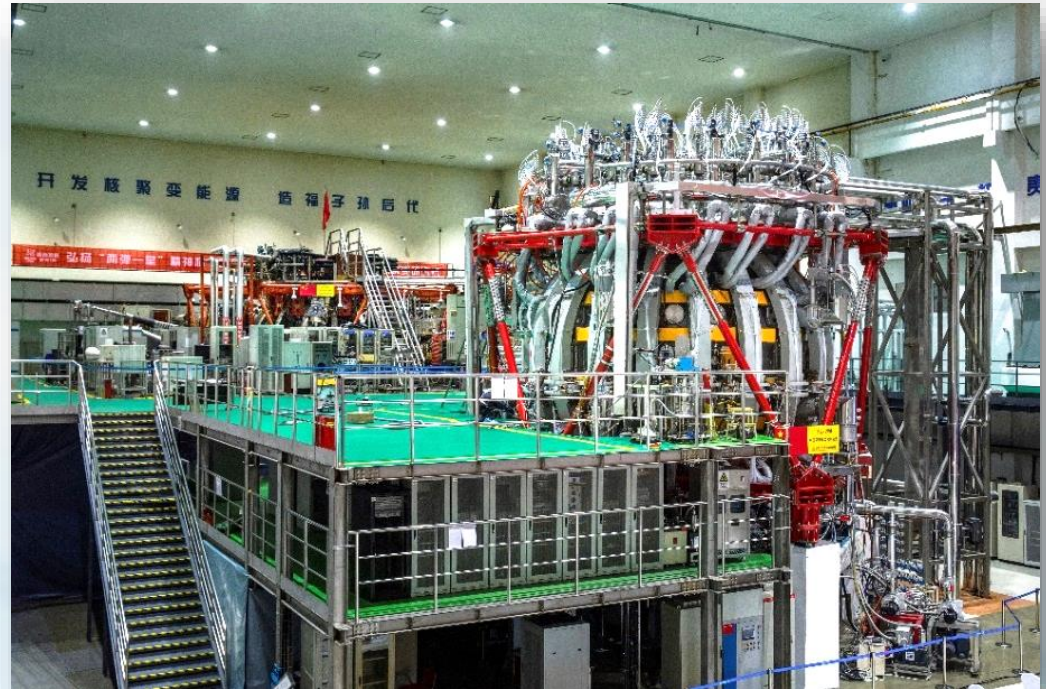
HL-2M Mission

Addressing critical physics and technology issues for ITER and next-step fusion devices

- High performance, high β_N scenarios compatible with flexible advanced divertor configurations, including Snow Flake (SF) and Tripod
- Tests and validation of high heat flux plasma-facing components
- Investigation of advanced plasma physics with high performance

Main Parameters

Major radius	$R = 1.78 \text{ m}$
Minor radius	$a = 0.65 \text{ m}$
Plasma current	$I_p = 2.5 \text{ (3) MA}$
Aspect ratio	$R/a = 2.8$
Elongation	$K = 1.8-2$
Triangularity	$\delta > 0.5$
Toroidal field	$B_T = 2.2 \text{ (3) T}$
Flux swing	$\Delta\Phi = 14\text{Vs}$
Heating power	25 (27) MW (NBI 15+EC 8+LH 2(4))



Magnets System and Vacuum Vessel

Demountable TF coils

- 20 TF coils
- Maximum 3T at 190kA

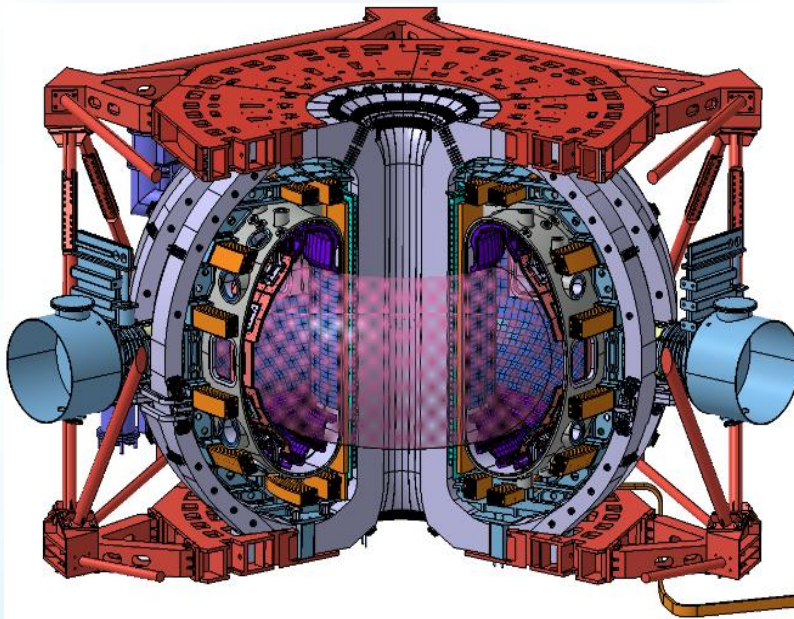
PF coils

- 17 PF coils
- Between VV and TFC

Vacuum Vessel :

- Double-shell structure
- Baking at 300 °C
- 42 m³

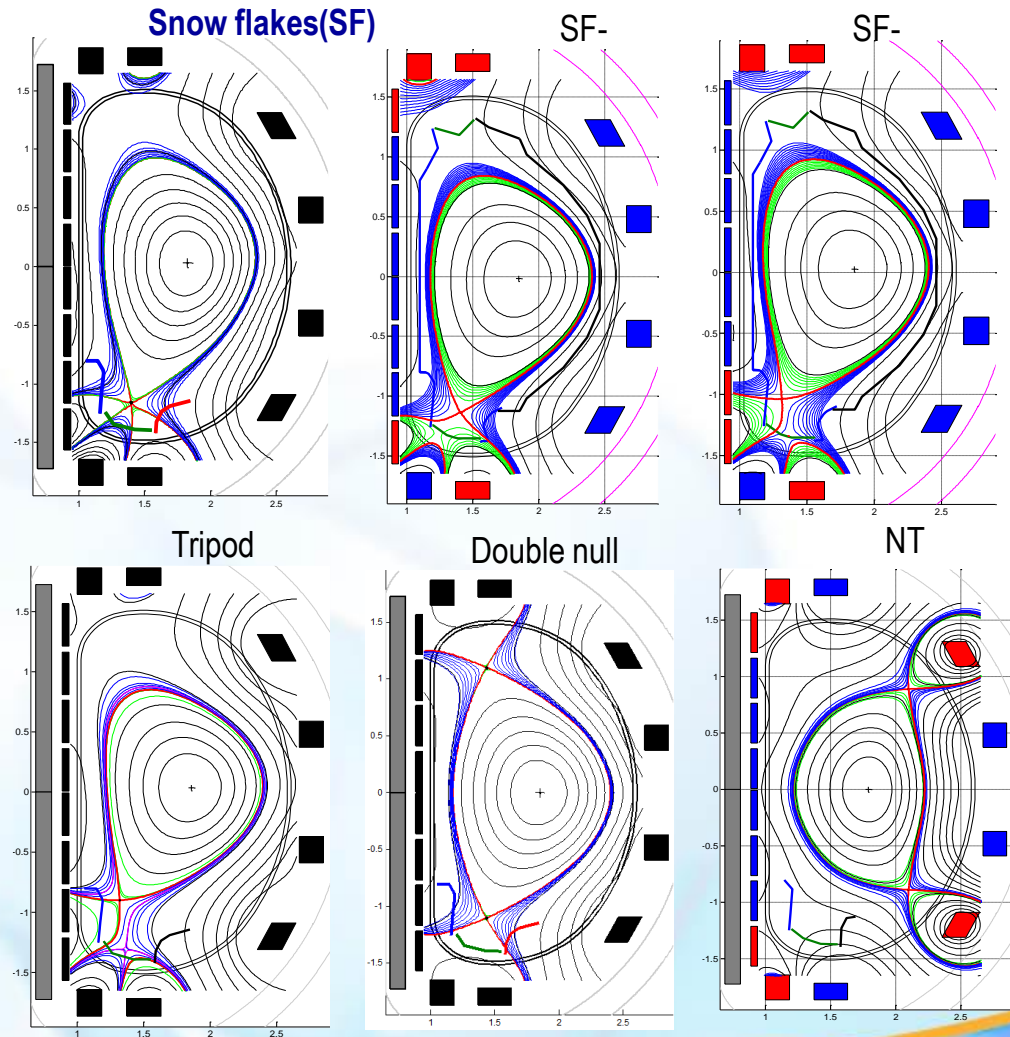
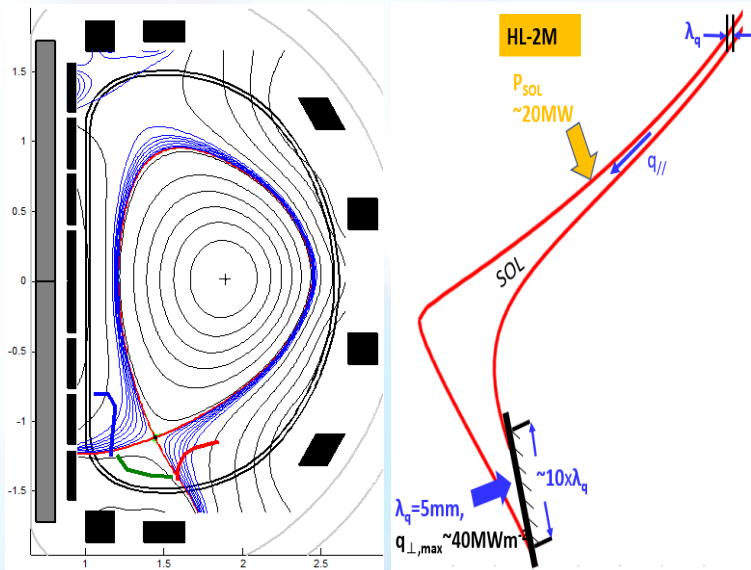
Coils System of HL-2M



Flexible Configurations

- Standard divertor with 14 MW/m² heat flux
- Advanced divertor configurations with Mega-Ampere plasma
- Heat flux width λ_q : 1~10mm

Standard divertor



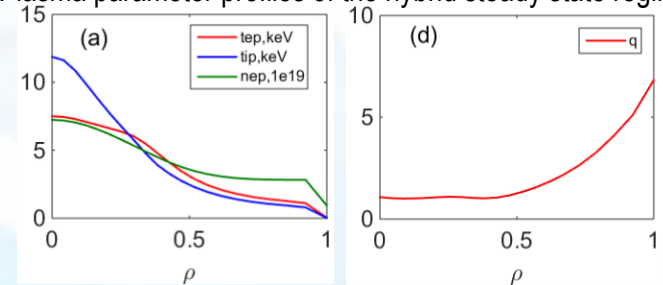
Advanced Scenarios with $I_p \geq 1\text{MA}$

In support of ITER pre-fusion phase operation (Hybrid and Steady State):

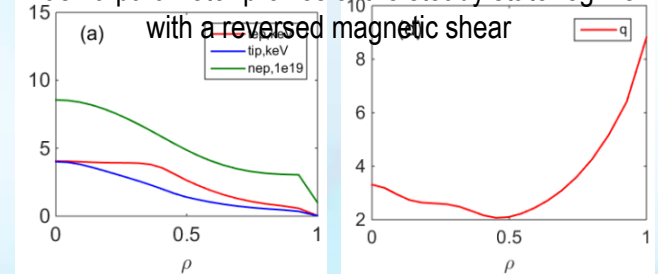
- Hybrid scenario : $I_p=1.0\sim 1.4\text{MA}$, $f_G \sim 0.5$ by combining NBCD with ECCD or ECCD+LHCD
- In Hybrid regimes, the fractions of bootstrap current f_{BS} and total non-inductive current f_{ni} are between 30%~45% and 70%~90%, respectively; β_N can reach 2.5 with $H_{98(y,2)} \sim 1.1$
- Full non-inductive regimes, such as the hybrid steady state regime and the regime with a reversed magnetic shear, can reach 1MA plasma current with $f_{BS} > 60\%$, $H_{98(y,2)} \sim 1.3$, $\beta_N > 3$.

	Hybrid			Full non-inductive	
$I_p(\text{MA})/B_z(\text{T})$	1.4/2.2	1.0/2.0	1.0/2.0	1.2/1.7	1.0/1.85
κ/δ	1.8/0.5	1.8/0.5	1.8/0.5	1.8/0.5	1.8/0.5
$a/R(\text{m})$	0.65/1.78	0.65/1.78	0.65/1.78	0.65/1.78	0.65/1.78
f_G	0.47	0.5	0.5	0.5	0.73
$P_{NBI}/P_{ECC1}/P_{LH} (P_{ECC2})$	10 /5 / (2)	6 /7 / (1)	6 /6 /3	10 /5.5 /-	1.5 /3.5 /4
X_{EC}/X_{LH}	0.34 / (0.28)	0.4 / (0.2)	0.3 /0.7	0.42 /-	0.45 /0.6
q_{95}	5.5	4.8	4.7	5.1	4.8
q_0/q_{min}	1.10 /0.80	1.10 /1.00	0.93 / 0.88	1.0 /1.0	1.10 /1.00
β_p	1.3	1.7	1.6	1.8	1.9
$\beta_N/4I_i$	2.3 /3.8	2.5 /3.9	2.4 /3.4	3.4 /4.0	2.3 /3.2
f_{BS}/f_{ni}	0.33 /0.76	0.40 /0.86	0.41 /0.89	0.55 /1.00	0.63 /1.00
Te_0/Ti_0 (keV)	8.4/9.2	6.7 /6.1	6.5 /5.8	7.5/12.0	4.0 /4.0
W_{th} (MJ)	1.3	0.85	0.82	1.3	0.95
$H_{98(y,2)}$	1.05	1.1	1.03	1.29	1.32

Plasma parameter profiles of the hybrid steady state regime



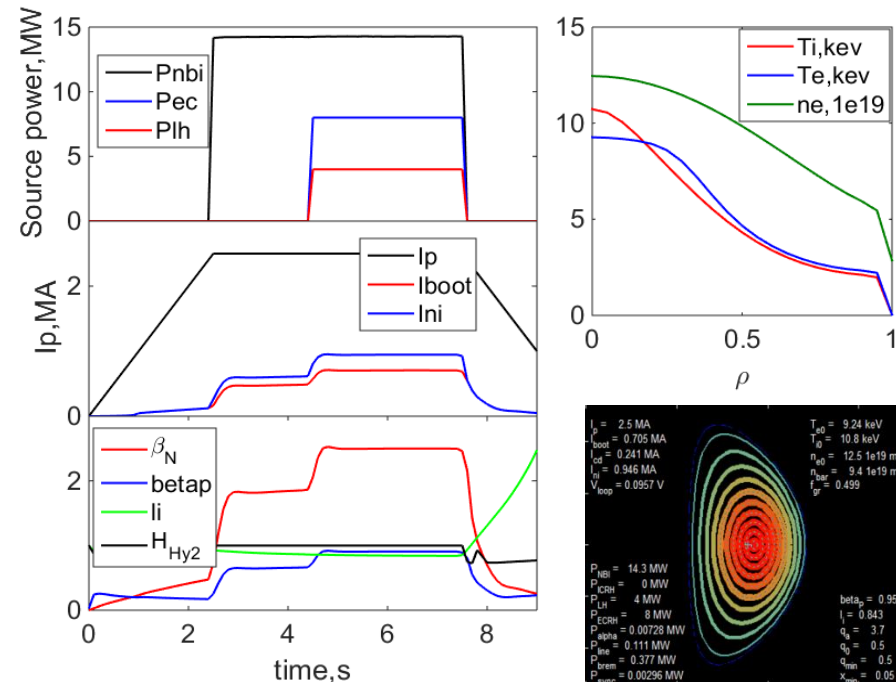
Plasma parameter profiles of the steady state regime with a reversed magnetic shear



High Performance at $I_p=2.5\text{MA} / B_t=2.2\text{T}$

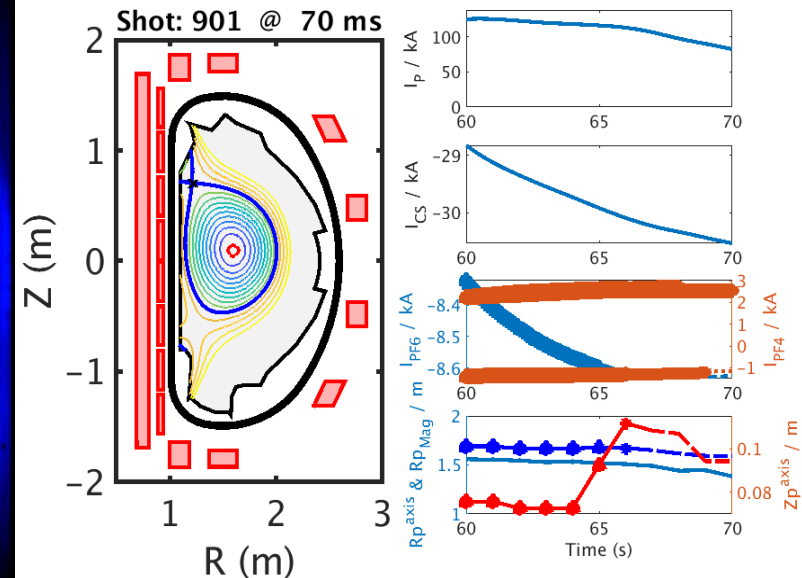
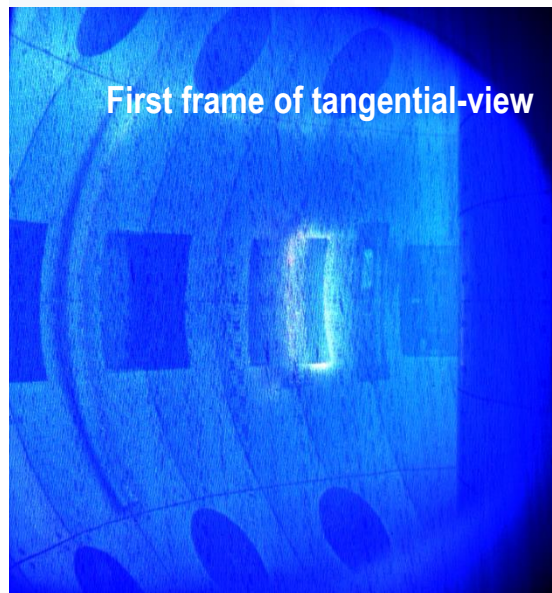
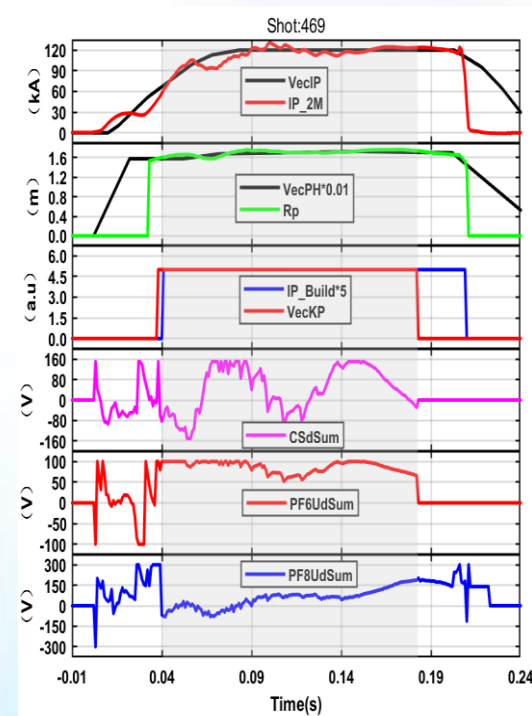
- High performance operation with $\beta_N \sim 3$ ($P_{\text{heat}} \sim 25\text{MW}(27\text{MW})$)
- $n(0) \tau T_i(0)$ can reach about $10^{20} \text{ m}^{-3}\text{skeV}$
- Central plasma temperature can reach around 10keV, with $f_G=0.5$

$I_p(\text{MA})/B_t(\text{T})$	2.5/2.2	2.5/2.2	2.5/2.2
κ/δ	1.8/0.5	1.8/0.5	1.8/0.5
$a/R(\text{m})$	0.65/1.78	0.65/1.78	0.65/1.78
f_G	0.6	0.6	0.5
$P_{\text{NBI}}/P_{\text{EC}}/P_{\text{LH}}$	15 / 8 / 2	15 / 8 / 4	15 / 8 / 4
$X_{\text{EC}}/X_{\text{LH}}$	0.3 / 0.7	0.3 / 0.7	0.3 / 0.7
q_{95}	3	3	3
β_p	0.98	1.00	0.95
$\beta_N/4I_i$	2.8 / 3.6	2.9 / 3.5	2.8 / 3.4
$f_{\text{BS}}/f_{\text{ni}}$	0.26 / 0.32	0.28 / 0.35	0.28 / 0.37
T_{e0}/T_{i0} (keV)	8.5/9.2	8.7 / 9.4	9.2 / 11
$T_{\text{eped}}/T_{\text{iped}}$ (keV)	1.5 / 1.4	1.6 / 1.5	2.2 / 2
$n_{\text{eped}}/n_{\text{sep}}$ ($1e19$)	7.3 / 4.1	7.3 / 4.1	5.4 / 2.9
W_{th} (MJ)	3.3	3.5	3.3
$H_{98}(y,2)$	1	1	1



HL-2M First Plasma

- First plasma achieved in 2020.
- Close-loop feedback control of plasma current and position was successfully implemented
- Divertor configuration realized.



H&CD and Diagnostic System

Auxiliary Heating

	NBI	ECRH	LHW
Present	5MW	5MW	2MW
Plan	15MW	8MW	4MW



Diagnostic

Parameters	Diagnostics
Density	CO ₂ , MW interferometers
Electron temperature	ECE, Soft X-ray
Radiation	Ha, bolometer, Hard X-ray...
Impurity	VUV...
neutral gas pressure	Vacuum gauge...
magnetic field	magnetic coils...
...	CCD...

More diagnostics such as profile measurements(MSE, CXRS...), fast particles(SLIP,NPA, Neutron camera, FIDA...), turbulence measurement (BES, Doppler reflectometry...) and so on are in progress.



Summary

HL-2A experiment:

- High β_N operation with DTB;
- Impurity effect on transport and confinement (H-mode enhancement, impurity mode, TEM);
- L-H transition and ELM mitigation (Velocity shear and SMBI on L-H, RMP and LBO on ELM mitigation)
- Energetic particle and MHD instability (Interaction EP, MHD and turbulence, Disruption prediction and mitigation)

HL-2M tokamak, with $R=1.78\text{m}$, $a=0.65\text{m}$, $B_T=2.2\sim 3\text{ T}$, $I_p=2.5\sim 3\text{MA}$, achieved its first plasma in 2020;

Aiming at critical physics and technology issues for ITER & fusion reactors, provide the platform for:

- High performance plasmas study for next-step fusion devices;
- Flexible divertor configuration (snowflake, tripod, etc.);
- Test and validation of PFC under high heat and particle flux;
- Key issue such as mitigation of ELM, disruption, VDE, etc.



For further details relevant to this talk please refer to:

Presenter	Session, Time	Presenter	Session, Time	Presenter	Session, Time
M. Jiang	EX/4 13/05, 14:20	N. Zhang	P3 12/05, 08:30	L.M.Yu	P3 12/05, 08:30
G.Z. Hao	TH/2 11/05, 11:48	D. Li	P3 12/05, 08:30	W.L. Zhong	P3 12/05, 08:30
Z.Y.Yang	TH/7 15/05, 08:30	L. Xue	P2 11/05, 14:00	L.G.Zang	P3 12/05, 08:30
N.Wu	P3 12/05, 08:30	Y.P. Zhang	P3 12/05, 08:30	J.Wen	P3 12/05, 08:30
T.Long	P3 12/05, 08:30	Y.Liu	P3 12/05, 08:30	W.Chen	P3 12/05, 08:30
H.L. Du	P4 12/05, 14:00	G.L.Xiao	P3 12/05, 08:30		



Thank you all for your attention!

